Xi'an Shiyou Daxue Xuebao (Ziran Kexue Ban)/
Journal of Xi'an Shiyou University, Natural Sciences Edition
ISSN: 1673-064X
E-Publication: Online Open Access
Vol: 67 Issue 12 | 2024
DOI: 10.5281/zenodo.14550712

INSILICO IDENTIFICATION OF PROTEIN-PROTEIN INTERACTIONS AND STRUCTURE-BASED FUNCTIONAL ANNOTATION OF *CAJANUS CAJAN* TRYPSIN INHIBITOR BY TARGETING INTEGRIN αVβIII

UNZILA YASIN
Centre for Applied Molecular Biology, University of the Punjab, Lahore.

ALEENA SUMRIN *
Centre for Applied Molecular Biology, University of the Punjab, Lahore. *Corresponding Author

Abstract

In this insilico work, we aim to explore the anti-angiogenic potential of *Cajanus cajan* trypsin inhibitors with pro-cancerous integrin αVβIII receptor based on protein-protein interaction approach. The study design was optimized to predict the best lead trypsin inhibitor molecule from a list of 12 proteins from *Cajanus cajan* (CcTI-1 to CcTI-12) retrieved via NCBI database and structured using C-I-TASSER, Alpha fold, Raptor X, and Tr-Rosetta servers. The best ranked 3D-structures from Alpha Fold with C-score -1.1- to -1.36 were validated using ramachandran plot >90% favored region, errat ~80%, and verify3D with ~86% score. Docking of CcTIs against integrin αVβIII (PDB ID: 3IJE) was carried out by ClusPro, PatchDock, ZDock, HDOCK, and HADDOCK servers. The highest negative Δ^iG and better interface interaction by PDBePISA suggested CcTI-11 x integrin αVβIII from PatchDock and CcTI-9 x integrin αVβIII from ZDock with Δ^iG of -6.9 and -16.7 and interface energies of 2634.4 and 1735.9 as best two docked complexes. Docking stability analysis of CcTI-9 and CcTI-11 docked structures by simulations at 100ns resulted in rmsd, rmsf, and gyration values to be 0.833nm and 0.342nm, 0.186nm and 0.126nm, 4.2nm and 4.1nm. Conclusively, better structural stability, less fluctuation, high compactness, and a higher hydrogen bonding, predicted CcTI-11 protein (accession no. >trIAOA151QRM2) to have a stronger binding with integrin αVβIII, a possible down-regulator of the receptor.

Keywords: Trypsin Inhibitor, *Cajanus Cajan*, Protein-Protein Docking, Integrin αvβiii, Molecular Dynamic Simulations.

1. INTRODUCTION

Structural insights into plant proteomics and molecular biology signify the importance of protein-protein interactions (PPIs) as the basis of different biological and physiological functions. There are ~650,000 or more PPI networks in humans involved in the signaling of bio-molecular, enzymatic, metabolic pathways, etc.

This biological interaction among proteins and other peptides, receptors, biomolecules, etc. predetermines how a gene transcribes into mRNA and eventually expresses as a mature protein. In some instances, certain PPIs lead to cancers, found part of invadopodia formation, cell invasion, cell migration, cell proliferation, and tumor prognosis (Clara *et al*., 2020).

This initial cellular identification is possible by computational analysis investigating the hidden cellular binding patterns, interface amino acid residues, and active pockets of the proteins (Cheng *et al*., 2020).

Xi'an Shiyou Daxue Xuebao (Ziran Kexue Ban)/
Journal of Xi'an Shiyou University, Natural Sciences Edition
ISSN: 1673-064X
E-Publication: Online Open Access
Vol: 67 Issue 12 | 2024
DOI: 10.5281/zenodo.14550712

Research in ethno-pharmacology has stated the high pharmacological impact of trypsin inhibitors (TIs) in therapeutics. These are defensive proteins with high binding affinity to cell adhesion molecules and receptors on cancer cells. Plant trypsin inhibitors harbor or hinder adhesion, migration and tumor invasion of cancerous cells activated via binding to different receptors like Src kinase, integrin, VEGFR, etc. (Abu-Darwish *et al*., 2018).

Antagonistic to proteases, trypsin inhibitors harbor initiation as well as metastatic stages of cancer by negatively regulating angiogenesis. These enzymatic inhibitors have interaction affinity towards their pre-destined gene targets, translating their biological functions in vitro (Soreide *et al*., 2006; Rasouli *et al*., 2017).

In this study, we determined the structural integrity, binding efficiency, and docking stability of *Cajanus cajan* trypsin inhibitor with integrin assuming the possible biological effect the protein might express in the cell upon interaction with the precancerous receptor (De Paula *et al*., 2012).

Molecular and structural evaluation of the functional relationship of proteins holds quite a significance in therapeutics and plant pharmacology. Biological molecules like proteins have a pre-destined function to perform in the cell; this function is largely dependent upon their cellular structure and interaction with each other.

If the structure of an unknown protein is available and analyzed for the intricate protein-protein binding, the native biochemical function can be predicted by homology modeling before confirming it experimentally.

Computational approaches are introducing new ways to deal with connect proteins with therapeutics. Sometimes, the preliminary sequence encoding the amino acids of a protein is enough to attain structural knowledge and predict the downstream functional properties through artificial learning methods.

These are usually the potential gaps in the correlation between the structural designing and characterization of plant trypsin inhibitors with the peculiar biological action it plays within a cell (Rastija *et al*., 2021, Castrosanto *et al*., 2023).

Plant trypsin inhibitors are reported to possess anti-proliferative properties. These trypsin enzymatic inhibitors exhibit interaction affinities towards integrin αVβIII, a receptor stimulating angiogenesis in the presence of proteases.

The structural interaction between trypsin inhibitors and integrin is important to understand the hidden inhibitory mechanism of trypsin inhibitors to predict the underlying cellular behavior. Although insilico findings are preliminary steps for the identification of new medicinal drugs clinical approval requires validation by in vitro results.

This broad spectrum analysis of proteins ranging from insilico to in vitro studies provides enough evidence to render it as a potential drug candidate for clinical studies against human diseases. In this study, we conducted insilico analysis on 12 different trypsin inhibitors from *Cajanus cajan*, ranging in size from 12-19kDa (Kumara *et al*., 2016, Shamsi *et al*., 2018, Shamsi *et al*., 2017).

Xi'an Shiyou Daxue Xuebao (Ziran Kexue Ban)/
Journal of Xi'an Shiyou University, Natural Sciences Edition
ISSN: 1673-064X
E-Publication: Online Open Access
Vol: 67 Issue 12 | 2024
DOI: 10.5281/zenodo.14550712

The retrieved sequences of trypsin inhibitors (CcTIs) were the templates for 3D-structure determination, structure validation, and docking with integrin αVβIII receptors, exploring their anti-cancer function on a molecular basis, later, assessed for stability by simulations.

Such computational prediction of the biological role relying on the structural linkage of trypsin inhibitors and cell surface receptors (integrin) reveals the molecular inhibitory mechanisms of inhibitors in cancer therapies. Currently, the insilico conclusions are being investigated by the experimental tests to confirm whether the structural or functional results align or not.

2. METHODOLOGY

2.1 Retrieval of *Cajanus cajan* trypsin inhibitor (CcTIs) sequences

The FASTA sequences of 12 different trypsin inhibitors from the *Cajanus cajan* plant (CcTIs) were retrieved from the NCBI (https://www.ncbi.nlm.nih.gov/) database. The accession number, protein size, and physiological properties of trypsin inhibitors were also recorded (Yousafi *et al*., 2019).

2.2 Phylogenetic analysis and MSA by MEGA X 6.0 software

To identify the phylogenetic analysis and multiple sequence alignment (MSA) of *C. cajan* trypsin inhibitors, MEGA X 6.0 software (Molecular evolutionary genetics analysis) was used. The conserved sequence and phylogeny relationship through tree construction connecting a link between the proteins were analyzed (Mahmoud *et al*., 2021).

2.3 Physicochemical properties of CcTIs

The physicochemical properties of trypsin inhibitors (CcTIs) were determined using Expasy, ProtParam server. Data involving molecular weight, no. of atoms, isoelectric point, total no. of positively and negatively charged amino acids, instability index, aliphatic index, grand average value of hydropathicity (GRAVY), extinction coefficient, estimated half-life, etc. were the traits retrieved (Afolabi *et al*., 2022; Hossain *et al*., 2012).

SoluProt 1.0 server (https://loschmidt.chemi.muni.cz/soluprot/) was used to predict the possible cellular location of CcTIs protein expressions in *E. coli* host system based on solubility score (Shey *et al*., 2022). PredictProtein server (https://predictprotein.org/) was used for identifying the presence of disulfide bonds in CcTIs sequences along with the structural entities like alpha helices, beta strands, and loops (Zahid and Sarwar, 2023). Amino acid sequences of CcTIs were submitted as templates and parameters were computed.

2.4 3D structure prediction

The 3D structures of CcTIs were generated using structure predicting tools of C-I-Tasser (https://zhanggroup.org/C-I-TASSER/), Raptor X (http://raptorx.uchicago.edu/), Alpha Fold(https://colab.research.google.com/github/sokrypton/ColabFold/blob/main/AlphaFold2.ipynb) and Tr-Rosetta (https://yanglab.nankai.edu.cn/trRosetta/) with FASTA

Xi'an Shiyou Daxue Xuebao (Ziran Kexue Ban)/
Journal of Xi'an Shiyou University, Natural Sciences Edition
ISSN: 1673-064X
E-Publication: Online Open Access
Vol: 67 Issue 12 | 2024
DOI: 10.5281/zenodo.14550712

sequences of CcTIs submitted as templates. The 3D protein structures generated were visualized by Pymol (https://pymol.org/) (Madanagopal *et al*., 2022; Xu, 2019; Anishchenko *et al*., 2021).

2.5 Structure evaluation by Ramachandran plot and SAVES server

The 3D structures predicted for CcTIs were validated by Ramachandran plot (https://zlab.umassmed.edu/bu/rama/) and SAVES server (https://saves.mbi.ucla.edu/). Structures were analyzed for non-bonded atomic interactions by errat, stereo-chemical quality by procheck and compatibility of predicted 3D structure with native structure by Verify3D (Hasan *et al*., 2021), further refined by energy minimization tool, YASARA (http://www.yasara.org/minimizationserver.html) (Saleem *et al*.,).

2.6 Active site prediction

For protein-protein docking, the interactive (active) residues for CcTIs proteins as ligands and integrin αVβIII receptor were obtained via CPORT (https://alcazar.science.uu.nl/CPORT), a plugin tool of HADDOCK (Singh *et al*., 2019).

2.7 Molecular docking

For docking studies, CcTIs were ligands and integrin αVβIII (PDB ID: 3IJE) was receptor retrieved from protein data bank (https://www.rcsb.org/). Different docking algorithm tools were utilized to predict the possible interactions between CcTIs and integrin αVβIII receptor to determine the efficiency of binding affinity of proteins with cells bearing integrin (Dong *et al*., 2019). For blind docking, no amino acids of ligands and receptors were specified, however, for focused docking active and passive residues were given (Aguiar, 2021; Gaur *et al*., 2018).

2.7.1 Protein-protein docking

Five protein-protein docking tools of ClusPro (https://cluspro.bu.edu/), PatchDock (https://bioinfo3d.cs.tau.ac.il/PatchDock/), ZDOCK (https://zdock.umassmed.edu/), HDOCK

(http://hdock.phys.hust.edu.cn/) and HADDOCK (https://wenmr.science.uu.nl/haddock2.4/) were used to study the 3D structural interaction between CcTIs and integrin αVβIII receptor, generating multiple docked structures with varied binding conformations and energy scores (Iqbal *et al*., 2021).

The default programs of ClusPro, PatchDock, HDock, and ZDock docking servers were selected for blind docking (Uciechowska-Kaczmaryck *et al*., 2019; Roy and Menon, 2022; Yan *et al*., 2020), whereas, HADDOCK was used to carry out focused docking algorithm (Scafuri *et al*., 2021).

Blind docking utilizes the default features of docking programs with PDB input files, assessed by CAPRI parameters (Rosell and Fernandez-Recio, 2020). For focused docking, it is necessary to define the active and passive residues of protein partners (Arya, 2021).

Xi'an Shiyou Daxue Xuebao (Ziran Kexue Ban)/
Journal of Xi'an Shiyou University, Natural Sciences Edition
ISSN: 1673-064X
E-Publication: Online Open Access
Vol: 67 Issue 12 | 2024
DOI: 10.5281/zenodo.14550712

2.8 PDBePISA and PDBsum Evaluation

PDBePISA server, a docking evaluation algorithm ranking docked complexes on their solvation free energy gain ($\Delta^{i}G$) and interface interaction between ligands and receptor was used (Krissinel and Henrick, 2007). The top-ranked docking complexes from each server were templates for PDBePISA analysis, narrowing down the best protein-protein docked complexes (CcTIs x integrin) by negative delta G' and highest residual interaction at the interface (Castrosanto *et al*., 2023).

To identify the amino acid residues involved in chemical bonds (hydrogen bonds, non-bonded contacts, and salt bridges) between docking structures, PDBsum server was used (Suganthi *et al*., 2024).

2.9 Molecular dynamics simulation

The stability of the CcTIs-integrin αVβIII docked complexes were analyzed by subjecting it to molecular dynamic simulations for 100ns via GROMACS v.2019.4 server (Das *et al*., 2021). Before running simulations, energy minimization and equilibrium were adjusted throughout the system following 3 steps.

Position restraints were applied for both ligands and receptors for each of the systems for 100ns. NPT (no. of atoms, pressure, and temperature) ensemble at a constant pressure (1 bar) and temperature (300K) were applied as protein preparation wizards across the NPT equilibrium phase for refining the docking complex.

The crucial steps were assigning bond orders, solvation by water molecules, introducing hydrogen atoms, and forming disulfide bonds. After completion of 100ns MD simulations, the trajectories were calculated for various dynamic analysis such as rmsd, rmsf, radius of gyration (Rg), no. of hydrogen bonds, and secondary structural analysis by the inbuilt feature scripts of GROMACS. The comparison of initial and final frames of simulations was observed by superimposition of docked structures (Suganthi *et al*., 2024, Majumder *et al*., 2022).

3. RESULTS AND DISCUSSION

Trypsin inhibitor is a potentially therapeutic protein, studied at structural, molecular, biochemical, and biological levels to explore the underlying facts about the biomolecule. The insilico findings emphasized how the enzymatic inhibitors (CcTIs) recognize, target, and react to their receptor substrate (integrin αVβIII), proving its possible anti-proliferative effect (Eleftheriou *et al*., 2020).

3.1 Sequence retrieval of *Cajanus cajan* trypsin inhibitor (CcTIs)

Cajanus cajan trypsin inhibitor shows sequential homology with soya bean Kunitz trypsin inhibitor, the first identified protease inhibitor. The FASTA sequences of 12 CcTIs are given in Table 1.

Xi'an Shiyou Daxue Xuebao (Ziran Kexue Ban)/
Journal of Xi'an Shiyou University, Natural Sciences Edition
ISSN: 1673-064X
E-Publication: Online Open Access
Vol: 67 Issue 12 | 2024
DOI: 10.5281/zenodo.14550712

Table 1: *Cajanus cajan* trypsin inhibitors (CcTIs)

Name	Amino acids	Accession no.	FASTA sequence
CCTI-1	176aa	>AAV51976.1	MMVLKVCVLVLFLVGVTTANMRMPEIRGVWKVEYLEECPRLSPIAHPAVPTRKPVNWQP ICRLNHIGSHGKGNTRKYLAIITPIGNSVPHPMMMFRTPCTYVDAVINITGILHSELYKQNTNSI SFKIICLSSIEHFLISHLKNVYMQVGMRVLIKLDVIFVPPHISISTYLLEIKI
CCTI-2	204aa	>XP_020213156.1	MKVLAIFCLICFAFTFFIVTTGAAPEPVLDTSGQKLITGVKYYILPVTRGKGGGLTVASTSANN DTCPLFVVQEKLEVLKGTPVTFTPYNAKTGLILTSTDLNIRSYVTSSTCAKPPVWKLLKVLTGV WFLSTGGIEGNPGIDTIVNWFKIEKAEKDYVLSFCPSVCKCQTLCRELGIYVDDDGYKHLSLS DKVPSFRIMFKRA
CCTI-3	209aa	>XP_020213133.1	MKFSMAVPLCLSLLLALNTHPLLAAEPEAVVDKQGEPLRPGVGYYVFPLWADEGGLSLGPT RNKTCPLDVIRDPSFIGLPLTFSAPGFDYIPTLTDLKVDFPVSTICVQSNVWRLRKEGAGFWF VSADGNPNDITSKFKIERLEGEHAYEIYSFKFCPSVPGTLCAPVGTFVDTDGTKVMAVGDNI EPYYVRFQKASVNHEKNQAFSIV
CCTI-4	113aa	>XP_020219717.1	MELKAMVKVGLLLFLLGFTATTVEARFDPSSFMTQLLWNGDDGVKTATTACCDACSCTKSI PPQCRCEDVGETCHSACKTCFCTRSIPPQCRCADITDFCYEPCTNYVHNEVH
CCTI-5	155aa	>tr|A0A151SZ51	MVPVKRGSGGGIELVATGNETCPLTVVQSPNKASKGNPCLVASPILFPYITPNSPFQIIFAFV PTCAPTRLWTIVDGLPEGPAVKIGGYHNIRNGAFQIQKASQRGCNHYKLLFCLDDTCEDIG VYVDSEGNRRLVLTKNDPFLVQFQRVTSSTA
CCTI-6	107aa	>KYP42282.1	MMVLKGCFFLLLLVGVTTARMDLGILKSGHDQHHSSKACCDECRCTKSIPPQCHCLDMRL NSCHSACESCVCTFSNPAMCHCVDTTDFCYKPCKSHDDDEKDLMNRF
CCTI-7	115aa	>tr|A0A151TBK5	MELKKVVLVKAALLLFFICFTASVDARFDPGSFITQVFSNGDAIYNVKSTTTACCDKCFCTKS NPPQCQCNDVGETCHTACKLCVCALSYPPQCRCMDNTSFCYDKCDTSKPKAH
CCTI-8	184aa	>tr|A0A151R1S0|A0A151R1S0	LLLTLSFLLFAFSTNLLLSFSQGAEQVLDRYGKPLIAARKYYIVPGIFGPTGGGVGLGKTGNST CQLLGFIFIGLPLEIASEEKPQCATSSNWVAVVDDFPLKWVGIGGAKDHPGKKIITGSFNIQA FDASYKLLFCPTMSASASTCFDIGRYDDVGGRRLVLTKDHPYQVGFIVADATRSSID
CCTI-9	176aa	>tr|A0A151R6N6	MYGQVAVNGGTFYILPVIRGSGGGIELAATGNETCALSVVQSRNEVSKGKPVTITSPFRTFF LPQGTVSVGFIDVPTCASTPSTWTVVEGLSEGSAVKITGYDNTVSGGFIIEQGDYIHYSYKLS FCAFDTSVCQPIGTSSDGHGNKPLVLTDGNPFEFVLQKVSSSSSSACTASA
CCTI-10	199aa	>tr|A0A151SYZ4	MKGITTLLFSLFLLFGFTSYLPSATAFDVLDTDGKLLRNGGSYYVVPVKRGSGGGIELAATGN ETCPLTVVQSPNKASKGNPCLVLSSILFAYITPNFPFQINFASVPTCAPTLLWTVVDGLPEGP AVKIGGYRDARSGAFQVQKASHRGCNHYKLLFCLDDTCEDIGVYVDSEGNRRLVLTKNDPL LIQFQRVTSSTA
CCTI-11	190aa	>tr|A0A151QRM2	MFTLFLLCALTSAIADAMVTDRDGDALRNGGTYHILPLFGVKDGGIELATTGNESCPLSVVQ SPSGATFRGLPIRISSPYRVAYISEGLILSLAFASAPSCAPSPPKWTVVKGLPEGEAVKLPGYRS TVSGWFKIEKSSFEYLYKVVFCARGSDTCGDVGVSVDGGGVSRLVVTDDEGIFVEFMKGNS VDA
CCTI-12	199aa	>tr|A0A151SYZ1	MKSSTVLSIILLSAFIASTTAKLVLDVDGEPVENNVAAYYLMPDLMGKGGGIERVRTGKETC PLTVVQSPFEVVNGLPVKIASSLRSYFIPEDSKVRIGFSSSPECASNPWWTVVEGLPEGPAVK ISGGYESTVEGWFKIMSVSSSPKLNNYKLMFCAREDDSCENIGIHKDAKGNRRLVVTDKNP MVIQFVKVASSSA

Xi'an Shiyou Daxue Xuebao (Ziran Kexue Ban)/
Journal of Xi'an Shiyou University, Natural Sciences Edition
ISSN: 1673-064X
E-Publication: Online Open Access
Vol: 67 Issue 12 | 2024
DOI: 10.5281/zenodo.14550712

3.2 Phylogeny and MSA analysis by MEGA X software

The N-terminal sequence of *C. cajan* trypsin inhibitor exhibits >70% homology with inhibitors from other legume plants like Glycine max, *Vigna angularis*, *Vigna ungulate*, *Phaseolus vulgaris*, etc. (Haq and Khan, 2003). Findings from MALDI/TOF partial sequencing of *C. cajan* protease inhibitors showed 100% homology with legume inhibitors (Swathi *et al*., 2014). The phylogenetic tree by MEGA X software (Fig. 1a) indicated the ancestral relationship between 12 CcTI proteins with amino acid variants generated during the evolutionary timeline. CcTI-3 (>XP_020213133.1) was the root ancestor (Fig. 1) exhibiting polytomy, a close phylogeny existing between different yet relatively similar proteins. CcTI-5 (>trIAOA151SZ51) and CcTI-10 (>trIAOA1515YZ4) while CcTI-9 (>trIAOA15R16N6) and CcTI-12 (>trIAOA151SYZ1) sharing the same clade were paralogs to each other. All the CcTIs proteins were homolog partners, showing the evolution of new proteins from the same plant.

In the case of multiple sequence alignment, amino acids of 12 CcTIs sequences were highly non-conserved. The conserved regions were in different stretches of CcTIs with maximum homology seen at amino acid positions of 1, 2, 15, 19, 21, 22, 27, 30, 34, 35, 39-41, 43, 44, 46, 52-55, 60, 64, 66-73, 78, 80, 81, 83, 107, 113, 115, 122, 133, 139, 145, 156, 172, 173, 183, 191, 194, and 196 (Fig. 1b).

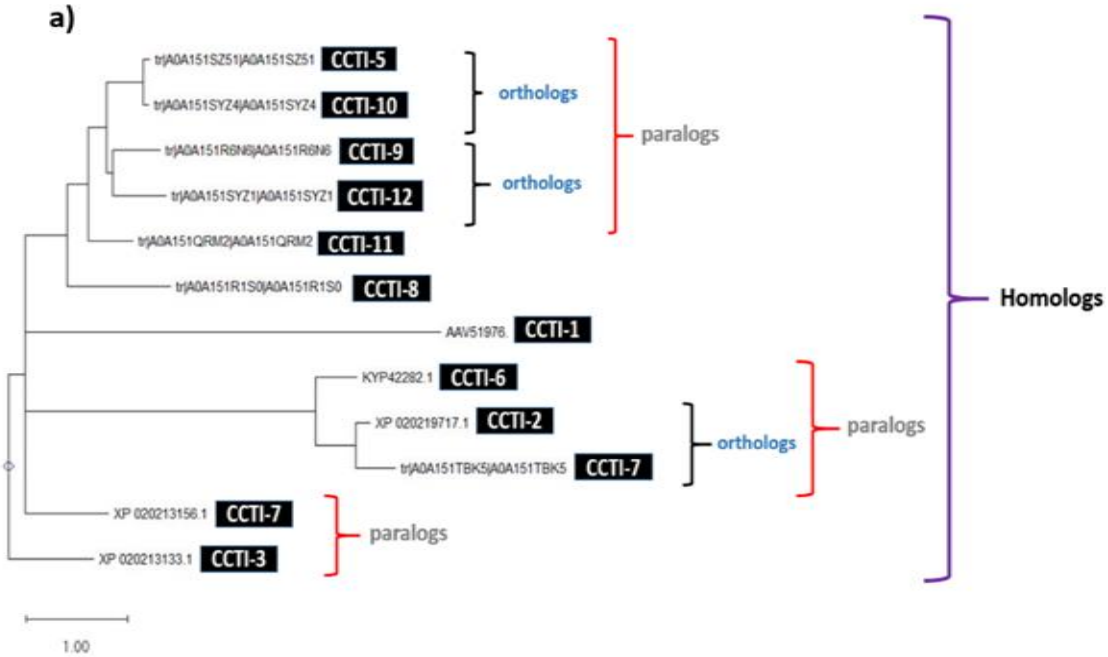

Xi'an Shiyou Daxue Xuebao (Ziran Kexue Ban)/
Journal of Xi'an Shiyou University, Natural Sciences Edition
ISSN: 1673-064X
E-Publication: Online Open Access
Vol: 67 Issue 12 | 2024
DOI: 10.5281/zenodo.14550712

b)

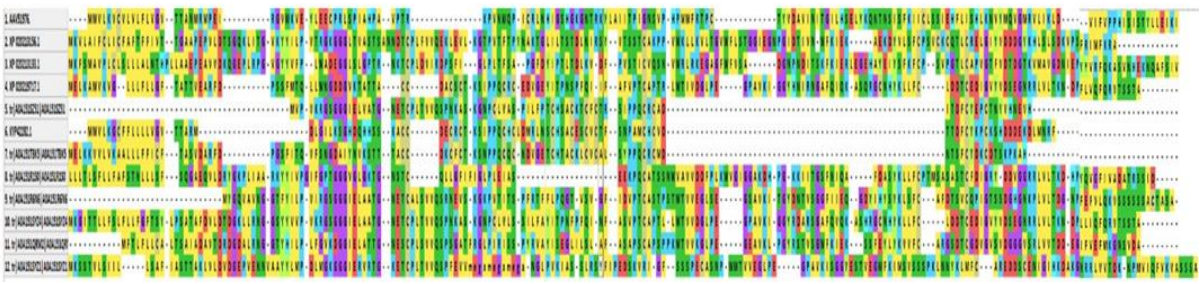

Figure 1: (a) Phylogenetic tree and (b) Multiple sequence alignment of 12 CcTIs proteins sequences using MEGAX 6.0 server

Table 2: Amino acids composition of CcTIs

Amino acids	CCTI-1	CCTI-2	CCTI-3	CCTI-4	CCTI-5	CCTI-6	CCTI-7	CCTI-8	CCTI-9	CCTI-10	CCTI-11	CCTI-12
Ala	2.8%	4.9%	6%	7.1%	5.8%	3.7%	7.8%	7.6%	5.7%	6.5%	7.9%	6%
Arg	4.5%	2.5%	3.3%	3.5%	4.5%	3.7%	1.7%	3.3%	1.7%	4%	4.2%	3.5%
Asn	5.1%	2.9%	3.8%	2.7%	5.8%	2.8%	4.3%	2.2%	3.4%	4.5%	1.6%	4.5%
Asp	1.1%	4.4%	5.7%	6.2%	3.9%	9.3%	7%	6%	3.4%	5%	5.8%	4%
Cys	2.8%	3.9%	2.4%	12.4%	3.9%	14%	13%	2.2%	2.8%	3%	2.6%	2%
Gln	1.7%	1.5%	1.9%	2.7%	4.5%	1.9%	3.5%	3.3%	3.4%	3%	0.5%	1%
Glu	4%	3.4%	5.3%	5.3%	3.2%	2.8%	1.7%	2.2%	4%	2.5%	4.7%	6.5%
Gly	4.5%	7.8%	7.7%	4.4%	9%	3.7%	2.6%	11.4%	11.9%	9.5%	11.5%	7.5%
His	4.5%	0.5%	1.4%	2.7%	1.3%	6.5%	1.7%	1.1%	1.1%	1%	0.5%	0.5%
Ile	11.9%	6.4%	4.3%	2.7%	6.5%	1.9%	2.6%	7.1%	5.7%	4%	4.7%	6%
Leu	9.7%	10.3%	9.6%	7.1%	7.7%	9.3%	6.1%	11.4%	5.1%	12.1%	8.9%	7%
Lys	5.7%	8.3%	5.3%	4.4%	4.5%	6.5%	8.7%	5.4%	3.4%	4.5%	4.2%	7%
Met	4.5%	1%	1.4%	2.7%	0.6%	5.6%	1.7%	0.5%	0.6%	0.5%	1.6%	3%
Phe	2.8%	5.9%	6.7%	5.3%	5.2%	4.7%	7%	7.1%	5.7%	6%	5.2%	3%
Pro	7.4%	5.4%	8.6%	5.3%	8.4%	3.7%	5.2%	4.9%	5.1%	6%	5.8%	6%
Ser	6.2%	6.4%	6.2%	5.3%	5.8%	8.4%	7%	8.2%	13.1%	7.5%	10.5%	12.1%
Thr	5.7%	10.3%	5.7%	11.5%	7.1%	5.6%	8.7%	6%	9.7%	8%	5.8%	4.5%
Trp	1.1%	1.5%	1.4%	0.9%	0.6%	0%	0%	1.1%	0.6%	0.5%	1%	1.5%
Tyr	3.4%	3.4%	3.3%	1.8%	2.6%	0.9%	2.6%	3.3%	3.4%	3.5%	3.1%	2.5%
Val	10.2%	9.3%	9.1%	6.2%	9%	4.7%	7%	6%	10.2%	8%	9.9%	11.1%

Xi'an Shiyou Daxue Xuebao (Ziran Kexue Ban)/
Journal of Xi'an Shiyou University, Natural Sciences Edition
ISSN: 1673-064X
E-Publication: Online Open Access
Vol: 67 Issue 12 | 2024
DOI: 10.5281/zenodo.14550712

3.3 Physiochemical properties of CcTIs

Structural properties of proteins are reflected on the physical, chemical, and biological properties. The isoelectric coefficient (pI) for CcTIs ranged from 5-9.5 graphically depicted in Fig. 2. The total no. of positively and negatively charged amino acid residues (Fig. 3) suggested that CcTI no. 1, 2, 5, 7, 8, and 10 were positively charged, CcTI no. 3, 4, 6, 9, and 11 were negatively charged, while CcTI 12 was neutrally charged.

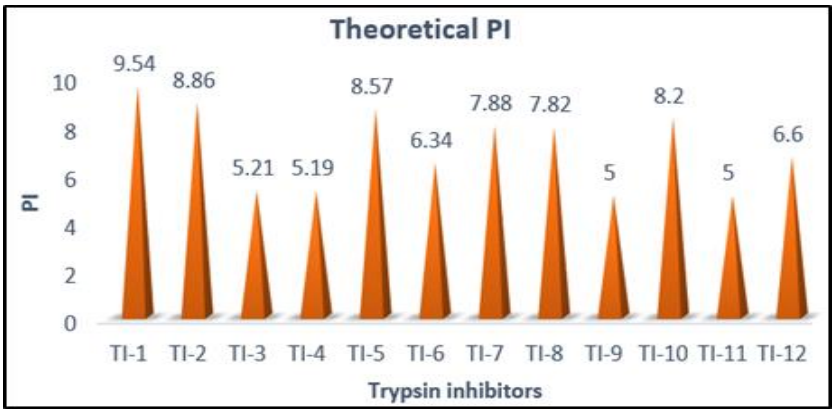

Figure 2: Isoelectric coefficient of C. cajan trypsin inhibitors

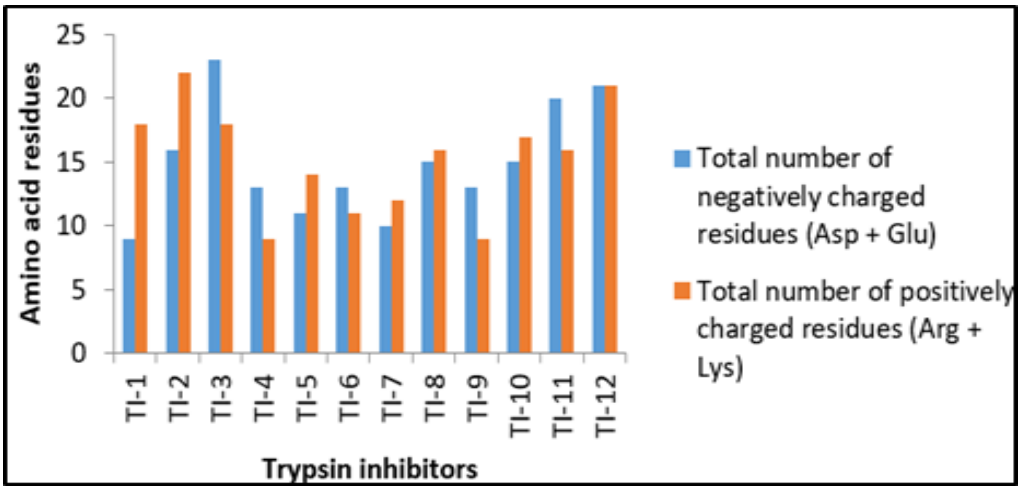

Figure 3: Total no. of +ive and -ive charged amino acids in C. cajan trypsin inhibitors

Trypsin inhibitors with instability index <40 are regarded as stable while the ones >40 are all unstable. CcTIs no. 1, 2, 3, 7, 8, 10, and 11 were stable while 4, 5, 6, 9, and 12 were unstable with index values exceeding 40 (Fig. 4). On the other side, the aliphatic index is the relative volume occupied by aliphatic side chains i.e. alanine, valine, isoleucine, and leucine. The higher the index value, the higher the thermostability of the protein's globular structure. Apart from trypsin inhibitors 4, 6 and 7, all other inhibitors were stable at high temperatures.

Xi'an Shiyou Daxue Xuebao (Ziran Kexue Ban)/
Journal of Xi'an Shiyou University, Natural Sciences Edition
ISSN: 1673-064X
E-Publication: Online Open Access
Vol: 67 Issue 12 | 2024
DOI: 10.5281/zenodo.14550712

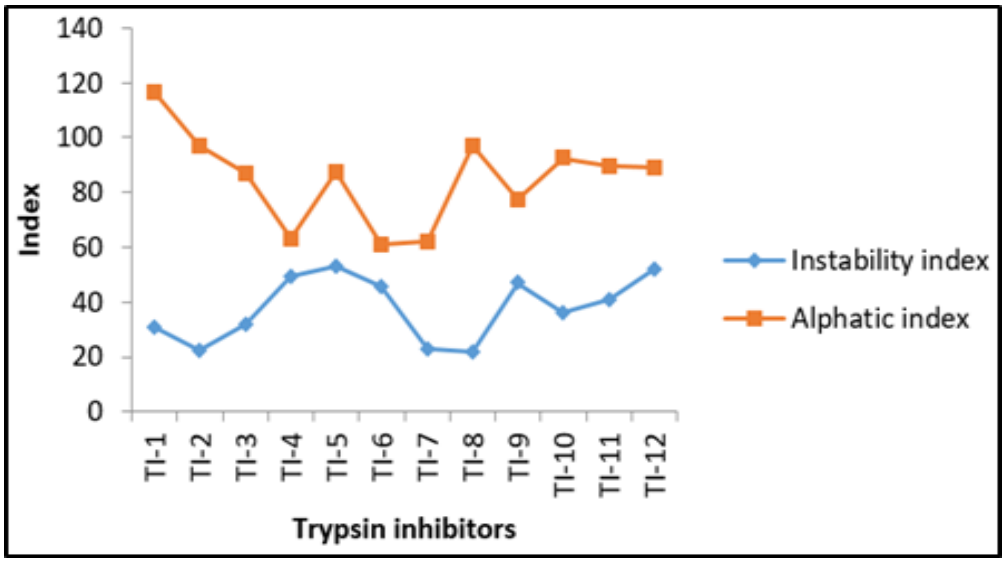

Figure 4: Instability index and aliphatic index of CcTIs

GRAVY i.e. grand average of hydropathicity identifies the hydrophilic and hydrophobic nature of proteins. In Fig. 5, trypsin inhibitors no. 3, 4, 5, 7, 9, 11, and 12 showed relatively higher GRAVY values compared to trypsin inhibitors no. 1, 2, 6, 8, and 10, exhibiting hydrophobic nature.

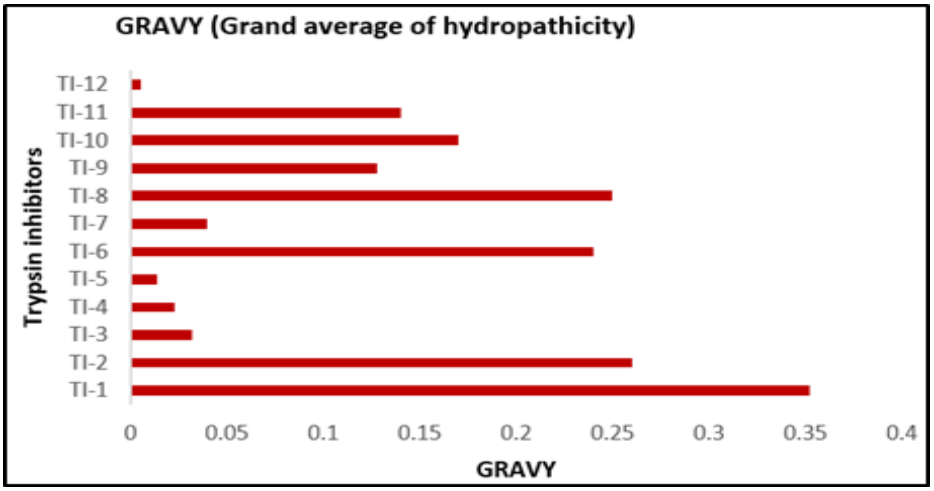

Figure 5: GRAVY values of C. cajan trypsin inhibitors

Xi'an Shiyou Daxue Xuebao (Ziran Kexue Ban)/
Journal of Xi'an Shiyou University, Natural Sciences Edition
ISSN: 1673-064X
E-Publication: Online Open Access
Vol: 67 Issue 12 | 2024
DOI: 10.5281/zenodo.14550712

Table 3: Physiochemical properties of trypsin inhibitors (CcTIs)

No. of Proteins	Molecular weight (Da)	No. of atoms	Theoretical PI	No. of negatively charged residues	No. of positively charged residues	Instability index	Aliphatic index	GRAVY
CCTI-1	19971.98	2872	9.54	9	18	30.96	116.7	0.352
CCTI-2	22356.23	3190	8.86	16	22	22.37	96.91	0.26
CCTI-3	22996.42	3233	5.21	23	18	31.97	87.18	0.032
CCTI-4	12447.33	1690	5.19	13	9	49.24	63.01	0.023
CCTI-5	16783.32	2364	8.57	11	14	53.1	87.35	0.014
CCTI-6	12014.97	1618	6.34	13	11	45.8	61.03	0.124
CCTI-7	12650.7	1730	7.88	10	12	23.18	61.91	0.04
CCTI-8	19750.78	2799	7.82	15	16	21.81	97.01	0.25
CCTI-9	18300.5	2543	5.01	13	9	47.02	77.44	0.128
CCTI-10	21436.62	3026	8.2	15	17	36.36	92.56	0.17
CCTI-11	20130.02	2828	5.24	20	16	40.00	89.79	0.13
CCTI-12	21526.79	3039	6.6	21	21	52.3	89.05	0.005

The solubility of CcTIs proteins in bacterial host predicted by SoluProt 1.0 server against the threshold value of < 0.5 suggested that apart from CcTI-3, CcTI-9, and CcTI-11, all other inhibitors showed insoluble expression in *E. coli*.

Table 4: Solubility prediction by SOLUPROT 1.0 server

Proteins	Accession Number	Solubility score	cellular expression
CCTI-1	>AAV51976.1	0.168	Insoluble
CCTI-2	>XP_020213156.1	0.175	Insoluble
CCTI-3	>XP_020213133.1	0.476	Soluble
CCTI-4	>XP_020219717.1	0.232	Insoluble
CCTI-5	>tr|A0A151SZ51	0.335	Insoluble
CCTI-6	>KYP42282.1	0.301	Insoluble
CCTI-7	>tr|A0A151TBK5	0.222	Insoluble
CCTI-8	>tr|A0A151R1S0	0.203	Insoluble
CCTI-9	>tr|A0A151R6N6	0.549	Soluble
CCTI-10	>tr|A0A151SYZ4	0.261	Insoluble
CCTI-11	>tr|A0A151QRM2	0.499	Soluble
CCTI-12	>tr|A0A151SYZ1	0.309	Insoluble

Xi'an Shiyou Daxue Xuebao (Ziran Kexue Ban)/
Journal of Xi'an Shiyou University, Natural Sciences Edition
ISSN: 1673-064X
E-Publication: Online Open Access
Vol: 67 Issue 12 | 2024
DOI: 10.5281/zenodo.14550712

The structural stability of proteins is markedly defined by the presence of the disulfide bond. PredictProtein server identified disulfide bonds in CcTI-4, CcTI-7, CcTI-8, and CcTI-12 proteins with a high frequency of beta strands and loops compared to helices.

Table 5: Disulfide bonds and parts of CcTIs tertiary structures by PredictProtein server

Proteins	No. of disulfide bonds	Location of bond	Alpha Helices	Beta strands	Loops
CCTI-1	0	-	16.5%	36.9%	46.6%
CCTI-2	0	-	7.8%	40.7%	51.5%
CCTI-3	0	-	6.2%	39.2%	54.5%
CCTI-4	6	(DB_bond: 55, 57) (DB_bond: 65, 67) (DB_bond: 74, 78) (DB_bond: 81, 83) (DB_bond: 91, 93) (DB_bond: 99, 103)	18.6%	14.9%	65.5%
CCTI-5	0	-	0%	51.0%	49.0%
CCTI-6	0	-	22.4%	10.3%	67.3%
CCTI-7	5	(DB_bond: 68, 70) (DB_bond: 77, 81) (DB_bond: 84, 86) (DB_bond: 94, 96) (DB_bond: 103, 107)	18.3%	13.0%	68.7%
CCTI-8	2	(DB_bond: 65, 87) (DB_bond: 137, 147)	4.9%	40.2%	54.9%
CCTI-9	0	-	0%	51.7%	48.3%
CCTI-10	0	-	8%	41.2%	50.8%
CCTI-11	0	-	0%	47.9%	52.1%
CCTI-12	2	(DB_bond: 62, 106) (DB_bond: 157, 164)	5.5%	41.2%	53.3%

3.4 Tertiary structure prediction of *Cajanus cajan* trypsin inhibitors (CcTIs)

Early protein identification as well as functional prediction of biomolecules has become quite easy and convenient using bioinformatics tools. In therapeutics, trypsin inhibitors as a chemopreventive or anti-inflammatory agent impede different stages of carcinogenesis.

The anti-tumor trypsin inhibitors reduce the growth incidence of tumorous cells by targeting G_0-G_1 phases or causing the arrest of S and G_2 phases affecting cell viability.

Previous insilico findings on computational identification of the possible biological potential of trypsin inhibitors hint that the active site of trypsin inhibitors have binding affinity to different substrates (Cid-Gallegos *et al*., 2022).

The tertiary structures for 12 trypsin inhibitor proteins obtained from four structure prediction tools i.e. C-I-Tasser, Alpha Fold, T-Rosetta, and Raptor X showed different structural poses with differently ranked energy scorings. The 3D protein models from C-I-Tasser and alpha fold had better C-score function (~-1.1- to -1.36) than T-Rosetta and Raptor X.

Xi'an Shiyou Daxue Xuebao (Ziran Kexue Ban)/
Journal of Xi'an Shiyou University, Natural Sciences Edition
ISSN: 1673-064X
E-Publication: Online Open Access
Vol: 67 Issue 12 | 2024
DOI: 10.5281/zenodo.14550712

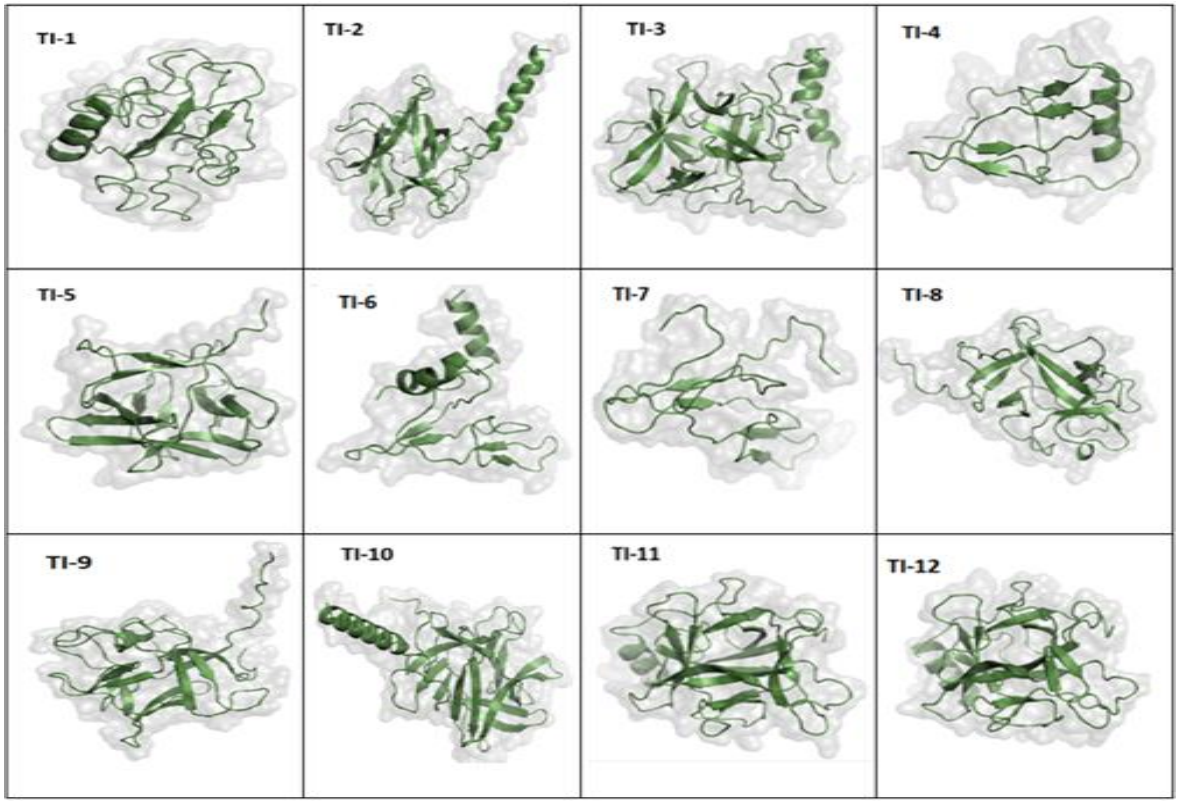

Figure 6: 3D structures of CcTIs proteins predicted by Alpha Fold server

On average, trypsin inhibitor structures were low in α-helixes (1-2 or no alpha-helix) and high on β-sheets (~10-12 β-sheets). Alpha helixes were formed between amino acid positions 5-15, 75-85, and 115-125 while β-strands were scattered in the trypsin inhibitor sequences. Alpha fold predicted 3D structures of 12 CcTIs proteins shown in Figure_6. A 2017 study on a 19kDa proteinase inhibitor from *C. cajan* focused on structure determination by C-I-Tasser and structural annotations of helixes, β-sheet, coils, and bond identifications (Shamsi *et al*., 2017).

In computational analysis, the Alpha fold server is the current gold standard in accurate structure prediction and is cited as number one in the most challenging and Critical Assessment of techniques for Protein Structure Prediction (CASP) experiments (Leppkes, 2022, Jumper *et al*., 2021). The insilico findings of Alpha Fold predicted protein structures were ranked as best models on energy scores, atomic placement, minimum outliers, and structural errors (Fig. 6).

3.5 Model validation and refinement

The 3D CcTIs structures with the highest %age of residues in the outlier of Ramachandran plot and poor quality by SAVES server were improved for atomic positioning, energy, and stoichiometry. A 3D structure of Tamarind trypsin inhibitor developed by Modeller resulted in high stability and less steric impediment using

Xi'an Shiyou Daxue Xuebao (Ziran Kexue Ban)/
Journal of Xi'an Shiyou University, Natural Sciences Edition
ISSN: 1673-064X
E-Publication: Online Open Access
Vol: 67 Issue 12 | 2024
DOI: 10.5281/zenodo.14550712

Ramachandran plot and SAVES (de Medeiros *et al*, 2021). The graphical evaluation by Ramachandran plot of CcTIs structures with >85% of residues in favored and 0-2% amino acid in disallowed region (Supporting info Figure S1). On average, errat score was ~80% and verify3D with ~86% of residues having 3D-ID-score > 0.1, rendering 3D CcTI protein models acceptable. A lower outlier indicate a better and more refined model compared to the native. The data from SAVES server is in Table 4.

Table 6: SAVES evaluation of 3D CcTI structures

SAVES parameters	Trypsin inhibitors	C-I-Tasser	Alpha Fold	Tr-Rosetta	Raptor X
Errat	CCTI_1	48.64%	73.05%	72.22%	43.2%
Verify 3D		71.79%	74.8%	52.25%	89.10%
Procheck		58.32%	58.5%	79.94%	76.83%
Errat	CCTI_2	98.27%	93.67%	94.44%	20.78%
Verify 3D		91.2%	93.96%	91.12%	17.09%
Procheck		63.87%	88.2%	89.54%	42.1%
Errat	CCTI_3	87.64%	74.01%	83.15%	43.76%
Verify 3D		83.01%	100%	92.80%	32.7%
Procheck		56.99%	81.9%	69.84%	11.6%
Errat	CCTI_4	72.5%	50.8%	93.33%	49.53%
Verify 3D		65.17%	71.45%	60.67%	69.21%
Procheck		59.32%	89.7%	84.2%	62.91%
Errat	CCTI_5	81.29%	85.71%	75.88%	58.32%
Verify 3D		85%	88.3%	84.52%	40.72%
Procheck		62.73%	89.7%	82.55%	44.72%
Errat	CCTI_6	91.54%	89.84%	89.87%	62.15%
Verify 3D		64.77%	63.68%	82.76%	49.62%
Procheck		66.27%	84.8%	82.89%	73.79%
Errat	CCTI_7	56.25%	86.81%	88.13%	52.91%
Verify 3D		64.17%	55.68%	45.45%	57.19%
Procheck		49.56%	88.81%	70.06%	62.39%
Errat	CCTI_8	78.3%	54.86%	75.57%	49.75%
Verify 3D		89.44%	100%	85.17%	57.48%
Procheck		59.99%	75.4%	65.98%	61.86%
Errat	CCTI_9	95.03%	92.85%	96.22%	66.82%
Verify 3D		88.64%	62.52%	92.61%	63.96%
Procheck		69.44%	85.4%	87.83%	50.77%
Errat	CCTI_10	92.77%	87.73%	89.30%	59.55%
Verify 3D		87.32%	98.85%	91.95%	53.73%
Procheck		50.88%	88.2%	77.45%	79.66%
Errat	CCTI_11	85.35%	93.5%	87.34%	49.99%
Verify 3D		100%	82.76%	98.28%	54.66%
Procheck		64.55%	92.8%	69.9%	73.55%
Errat	CCTI_12	93.45%	89.09%	89.28%	70.03%
Verify 3D		85.32%	92.66%	75.15%	68.32%
Procheck		63.74%	89.2%	77.39%	72.42%

Xi'an Shiyou Daxue Xuebao (Ziran Kexue Ban)/
Journal of Xi'an Shiyou University, Natural Sciences Edition
ISSN: 1673-064X
E-Publication: Online Open Access
Vol: 67 Issue 12 | 2024
DOI: 10.5281/zenodo.14550712

3.6 Active site prediction

Docking hugely rely on interacting (active) and non-interacting (passive) residues of ligands and receptors. The amino acid residues of CcTIs and integrin αVβIII were identified using CPORT server, given in table 4.7, figure 4.8 and 4.9.

Table 7: Positions of interacting amino acids of CcTIs structures by CPORT server

Proteins	Positions of interacting amino acid of CCTIs by CPORT
CcTI-1	25, 26, 27, 28, 29, 30, 40, 43, 50, 51, 52, 53, 54, 71, 81, 83, 85, 123, 124, 132, 136, 147, 149, 155, 156
CcTI-2	1, 2, 27, 28, 29, 46, 53, 54, 56, 66, 67, 68, 83, 88, 92, 98, 100, 101, 103, 105, 107, 114, 115, 116, 117, 118, 119, 120, 121, 124, 141, 143, 145, 146, 147, 148, 149, 150, 151, 152, 170
CcTI-3	1, 2, 3, 25, 26, 27, 28, 29, 30, 40, 43, 50, 51, 52, 53, 54, 71, 81, 83, 85, 123, 124, 132, 136, 137, 138, 139, 142, 162, 164, 165, 176, 177, 178, 179, 180, 181, 182, 183, 184, 185, 186
CcTI-4	1, 2, 5, 6, 9, 10, 14, 33, 34, 35, 36, 37, 38, 39, 40, 45, 46, 47, 48, 49, 51, 55, 57, 58, 59, 60, 61, 62, 63, 64, 65, 66, 68, 74, 75, 82, 83, 84, 85, 86, 87, 88, 89
CcTI-5	4, 5, 6, 37, 38, 39, 40, 41, 42, 43, 44, 45, 46, 47, 48, 49, 50, 51, 52, 53, 55, 57, 62, 65, 66, 68, 70, 71, 100, 101, 105, 106, 107, 108, 109, 146, 147, 148, 149, 150, 151, 152, 153, 154, 155
CcTI-6	1, 2, 3, 5, 6, 23, 24, 25, 26, 27, 28, 29, 30, 31, 32, 36, 37, 38, 39, 40, 41, 50, 51, 52, 53, 54, 55, 56, 57, 58, 59, 61, 63, 64, 65, 67, 68, 83, 84, 85, 86, 87
CcTI-7	1, 2, 3, 4, 5, 6, 7, 9, 11, 17, 18, 19, 20, 22, 27, 29, 30, 31, 32, 33, 34, 35, 36, 37, 39, 45, 46, 48, 49, 50, 51, 52, 53, 55, 56, 57, 58, 59, 60, 61, 62, 63, 64, 65, 66, 68, 70, 76, 78, 79, 80, 82, 83, 84, 85, 88
CcTI-8	1, 2, 3, 5, 7, 8, 9, 10, 14, 15, 19, 23, 24, 25, 26, 27, 28, 29, 30, 31, 32, 35, 49, 52, 55, 103, 104, 105, 106, 107, 109, 117, 118, 119, 120, 121, 122, 123, 147, 149, 157, 158, 159, 160, 161,
CcTI-9	1, 2, 3, 4, 5, 6, 7, 8, 10, 15, 16, 17, 18, 19, 20, 34, 46, 55, 57, 58, 59, 61, 62, 63, 65, 66, 74, 77, 78, 81, 82, 113, 114, 116, 117, 118, 119, 120, 122, 129, 130, 132, 133, 156, 160, 161, 162, 163, 168, 169, 170, 171, 172, 173, 174, 175, 176
CcTI-10	1, 2, 3, 5, 9, 10, 11, 13, 15, 16, 17, 38, 59, 61, 63, 64, 65, 66, 67, 68, 70, 72, 73, 74, 76, 84, 85, 111, 112, 114, 115, 119, 120, 122, 125, 136, 137
CcTI-11	1, 3, 5, 6, 7, 8, 9, 11, 12, 14, 21, 22, 23, 24, 25, 26, 47, 48, 49, 50, 62, 63, 66, 67, 69, 70, 83, 84, 87, 119, 120, 122, 123, 124, 125, 135, 161, 167, 168
CcTI-12	1, 12, 13, 14, 18, 20, 21, 22, 23, 24, 25, 26, 31, 48, 49, 50, 51, 52, 53, 55, 58, 60, 62, 63, 64, 65, 66, 67, 70, 71, 122, 123, 125, 126, 176, 177

Xi'an Shiyou Daxue Xuebao (Ziran Kexue Ban)/
Journal of Xi'an Shiyou University, Natural Sciences Edition
ISSN: 1673-064X
E-Publication: Online Open Access
Vol: 67 Issue 12 | 2024
DOI: 10.5281/zenodo.14550712

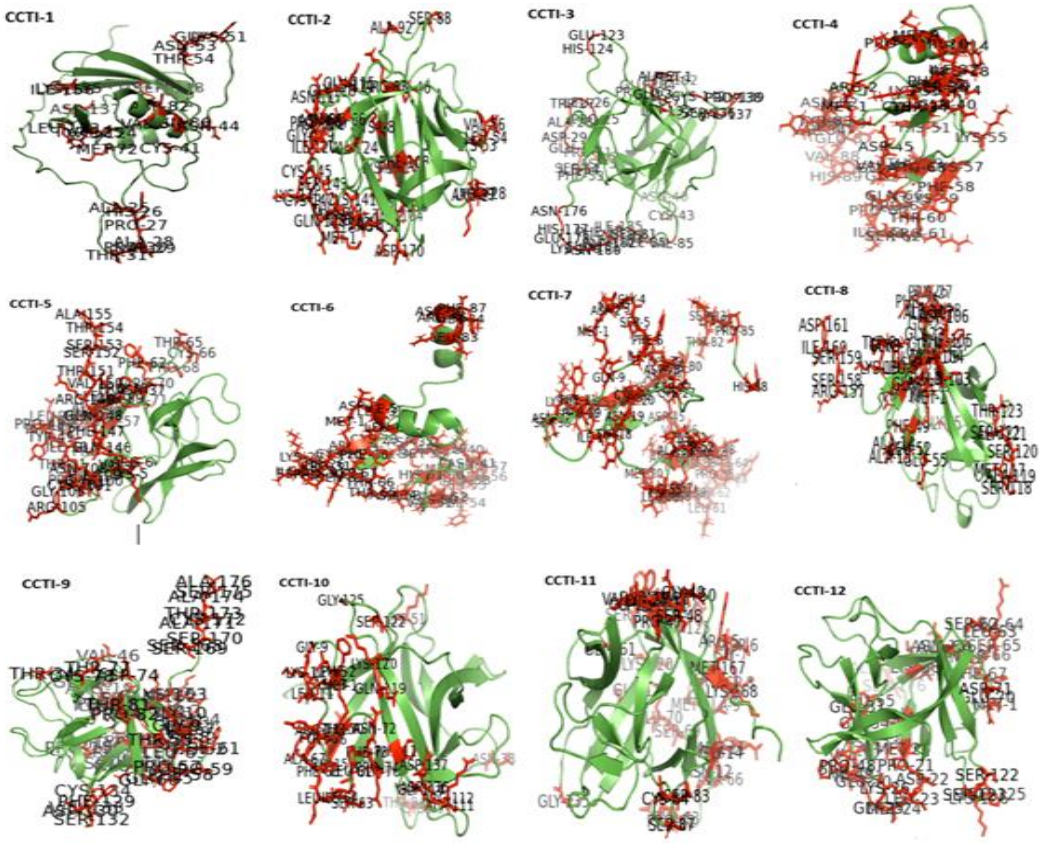

Figure 7: Interacting amino acids of CcTIs

a)

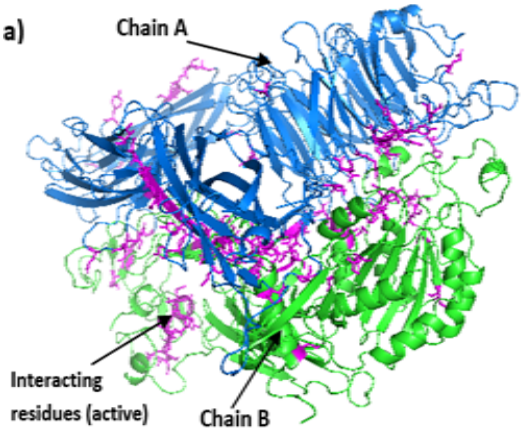

b)

Receptor	Interacting active amino acids by CPORT
Integrin αVβIII	91, 145, 150, 178, 179, 214-216, 218, 219, 221, 245, 248, 249, 272, 273, 305, 306, 308, 309, 325, 337, 367, 385, 386, 399, 450, 465, 467, 506, 654, 658, 659, 661, 749, 756, 758, 909, 911-917, 953-967, 1128, 1132, 1221-1224, 1226-1229, 1231-1233, 1250, 1251, 1441, 1442, 1444-1446, 1477, 1478, 1491, 1492, 1494-1500, 1502-1504, 1506, 1508-1511, 1513-1515, 1518-1522, 1524, 1525, 1548, 1557, 1611, 1612, 1615

Figure 8: (a) Integrin αVβIII receptor (b) Interacting amino acids of integrin αVβIII

3.7 Protein-protein docking

Integrin biomarkers are overexpressed on cancerous cells, exhibiting the modified cell behavior through gene expression profile, and the relation between tissue-resident cells

Xi'an Shiyou Daxue Xuebao (Ziran Kexue Ban)/
Journal of Xi'an Shiyou University, Natural Sciences Edition
ISSN: 1673-064X
E-Publication: Online Open Access
Vol: 67 Issue 12 | 2024
DOI: 10.5281/zenodo.14550712

and extracellular matrix (ECM). Cancer cells release proteases that have binding potential towards integrin, leading to cellular pathogenesis. To deal with such non-ideal cell conditions, disruption of ligand binding site by competitive binding of protease inhibitors to precancerous integrin in place of protease enzymes is a thought-provoking idea (Weis and Cheresh, 2011). Findings from protein-protein docking showed CcTIs proteins have binding affinity to both chains of integrin receptor (A and B), targeting the cleft binding sites. Beatrice S. Ludwig in 2021 docked integrin αVβ6 with sunflower trypsin inhibitor, harboring the elevated expression of receptor in breast and lung cancer metastasis, targeting a peptide domain to selectively induce anti-angiogenesis (Ludwig *et al*., 2021). This inhibitory nature of *Cucumis melo* TI with integrin αVβIII, speculates TI binding to the cleft of integrin receptor, down-regulating tumorogenesis (Mahnam, 2016). Inhibitors compete with proteases to bind the mobile domain of integrin, up-regulating expression of tumor suppressing genes and inactivating matrix metalloproteases, involved in invasion, migration, and invadopodia in cancers (Cid-Gallegos et al., 2022).

Table 8: Energy scores of top docked complexes (CcTIs x integrin αVβIII) from 5 docking algorithms

Cajanus cajan trypsin inhibitors	ClusPro	ZDock	PatchDock	HDock	HADDOCK
CCTI-1	-1078	1642	20778	-357	-0.5
CCTI-2	-1035	1702	22206	-288	-1.4
CCTI-3	-1108	2010	25894	-332	-2.5
CCTI-4	-1066	1636	23282	-364	-1
CCTI-5	-1136	1739	21186	-328	-1.9
CCTI-6	-1095	1865	20422	-382	-1.2
CCTI-7	-1078	1744	19838	-338	-0.1
CCTI-8	-1140	1521	22562	-307	-0.16
CCTI-9	-1155	1953	25560	-329	-1.6
CCTI-10	-1072	1803	22628	-339	-2.1
CCTI-11	-1191	1698	25040	-307	-1.6
CCTI-12	-925	1692	22466	-324	-1.4

3.7 PDBePISA and PDBsum evaluation

To study protein-protein interactions, Nielsen in 2022 identified the covalent networking of protease inhibitors by PDBePISA with interface surface area of 1380Å and $\Delta^{i}G$ *P*-value of 0.18 (Nielsen *et al*., 2022). The docking complexes (integrin αVβIII i.e. A and B chains and trypsin inhibitor i.e. C chain) were analyzed on the highest interface interaction and

Xi'an Shiyou Daxue Xuebao (Ziran Kexue Ban)/
Journal of Xi'an Shiyou University, Natural Sciences Edition
ISSN: 1673-064X
E-Publication: Online Open Access
Vol: 67 Issue 12 | 2024
DOI: 10.5281/zenodo.14550712

greater negative $\Delta^{i}G$ value by PDBePISA server (Castrosanto *et al*., 2023) ranking top 2 docking models for molecular dynamic simulations. Our PDBePISA findings concluded that CcTI-11 x integrin complex from Patch dock with an interface surface area (avg. 1460Å) is better than CcTI-9 x integrin (avg. 942Å) from ClusPro. On the other hand, CcTI-11 x integrin αVβIII docked complex had a relatively lower $\Delta^{i}G$ value (solvation energy) i.e. -6.9 and 0.2 compared to CcTI-9 x integrin αVβIII complex (Table 6), the 3D conformation given in Fig. 7.

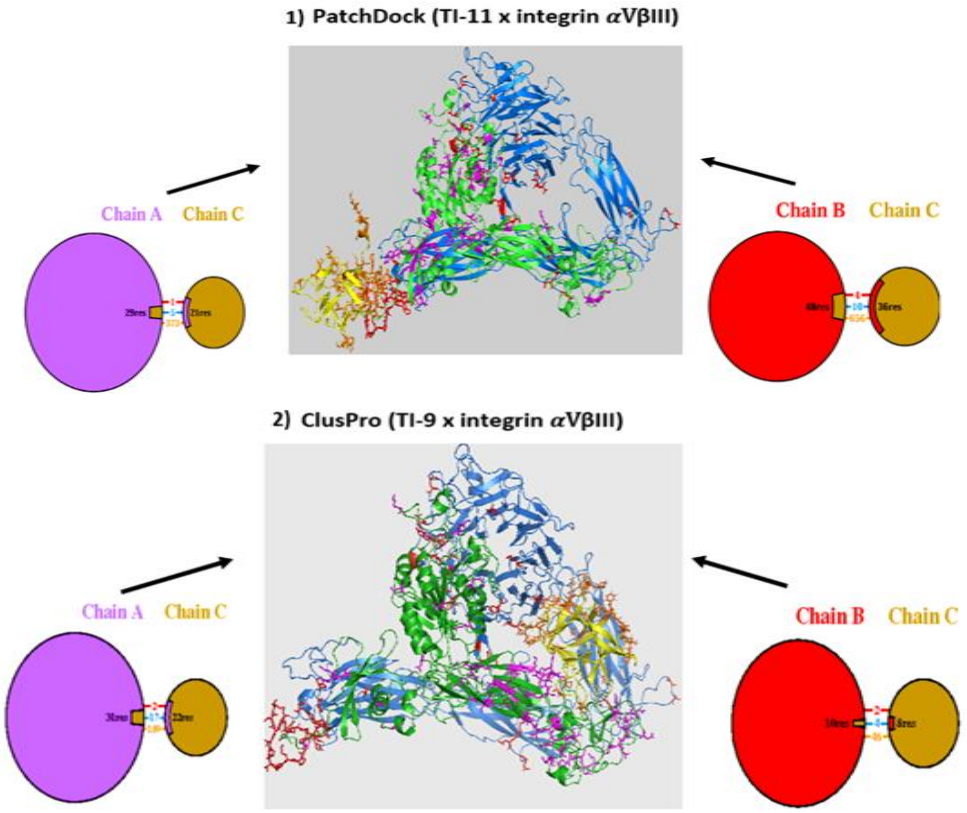

Figure 9: 3D-conformation of top 2 complexes with P-P interactions between the receptor (chain A and B) and ligand (chain C) by PDBsum server

Reports states that intermolecular interactions between different plant trypsin inhibitors were low in salt bridges and high in hydrogen bonds with Arg and Lys (Gartia *et al*., 2020). PDBsum server predicted that ClusPro docked CcTI-9 x integrin αVβIII was rich in hydrogen bonds while the PatchDock docked CcTI-11 x integrin αVβIII model had a high frequency of salt bridges (Table 6), thus, the frequency of H-bonds > salt bridges.

Arg, Ser, Tyr, and Lys residues of CcTIs and Arg and Glu of integrin receptor were involved in hydrogen bonding. Moreover, His, Glu, Leu, and Arg residues of CcTIs along with Lys and Cys of integrin αVβIII receptor were predominant in non-bonded contacts (Table 7).

Xi'an Shiyou Daxue Xuebao (Ziran Kexue Ban)/
Journal of Xi'an Shiyou University, Natural Sciences Edition
ISSN: 1673-064X
E-Publication: Online Open Access
Vol: 67 Issue 12 | 2024
DOI: 10.5281/zenodo.14550712

Table 9: PDBePISA and PDBsum predicted Δ^iG, Å2, H-bonds, and salt bridges in docked complexes

PDBePISA and PDBsum evaluation	PatchDock (CCTI-11 x integrin $\alpha V\beta III$)		ClusPro (CCTI-9 x integrin $\alpha V\beta III$)	
	A_C	B_C	A_C	B_C
Δ^iG (solvation energy)	-6.9	0.2	-16.7	-2.9
Å2 (Interaction at interface)	2634.4	285	1735.9	149.3
No. of hydrogen bonds	5	10	17	4
No. of salt bridges	1	4	2	2
Non-bonded contacts	373	656	189	46

Table 10: Protein-protein interactions within trypsin inhibitor (chain C) and integrin $\alpha V\beta III$ (chain A and B) docked complexes

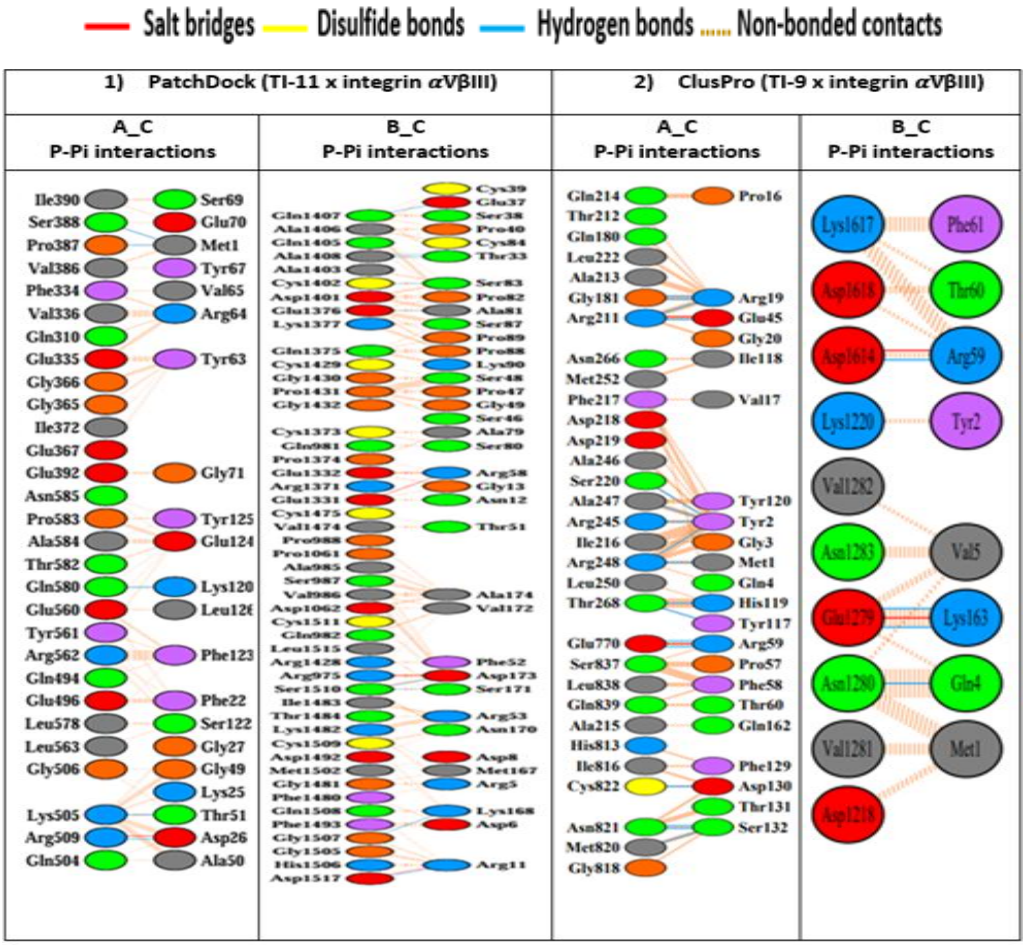

Xi'an Shiyou Daxue Xuebao (Ziran Kexue Ban)/
Journal of Xi'an Shiyou University, Natural Sciences Edition
ISSN: 1673-064X
E-Publication: Online Open Access
Vol: 67 Issue 12 | 2024
DOI: 10.5281/zenodo.14550712

3.8 Molecular dynamic simulations

PatchDock and ClusPro generated CcTI-11 and CcTI-9 docked complexes with integrin αVβIII receptor were chosen for simulations based on PDBePISA docking analysis. To address the stability concerns and changes in the structural conformations, the unbounded CcTIs proteins and their bound targets (CcTI x integrin αVβIII) were subjected to 100ns molecular simulations and appraised by parameters of rmsd, rmsf, no. of hydrogen bonds, and radius of gyration (Rg) (Castrosanto *et al*., 2023).

The CcTIs X integrin αVβIII complexes remained intact during simulation periods with minor structural changes in binding pose (Fig. 10a1 and 10a2 indicating CcTI-9 x integrin αVβIII at 0ns and 100ns while Fig. 10b1 and 10b2 indicating CcTI-11 x integrin αVβIII at 0ns and 100ns). The binding energies via simulations of CcTI-9 and CcTI-11 complexes with integrin receptor (TI x Integrin αVβIII) were -69.7 and -95.3 kcal/mol. The high -ive value represents stable binding free energy scores depicting equilibrated structural conformations of the protein-docked structures. The binding energetics of CcTI-9 with receptor was lower than that of CcTI-11, thus, reduced energy levels indicated a high binding affinity.

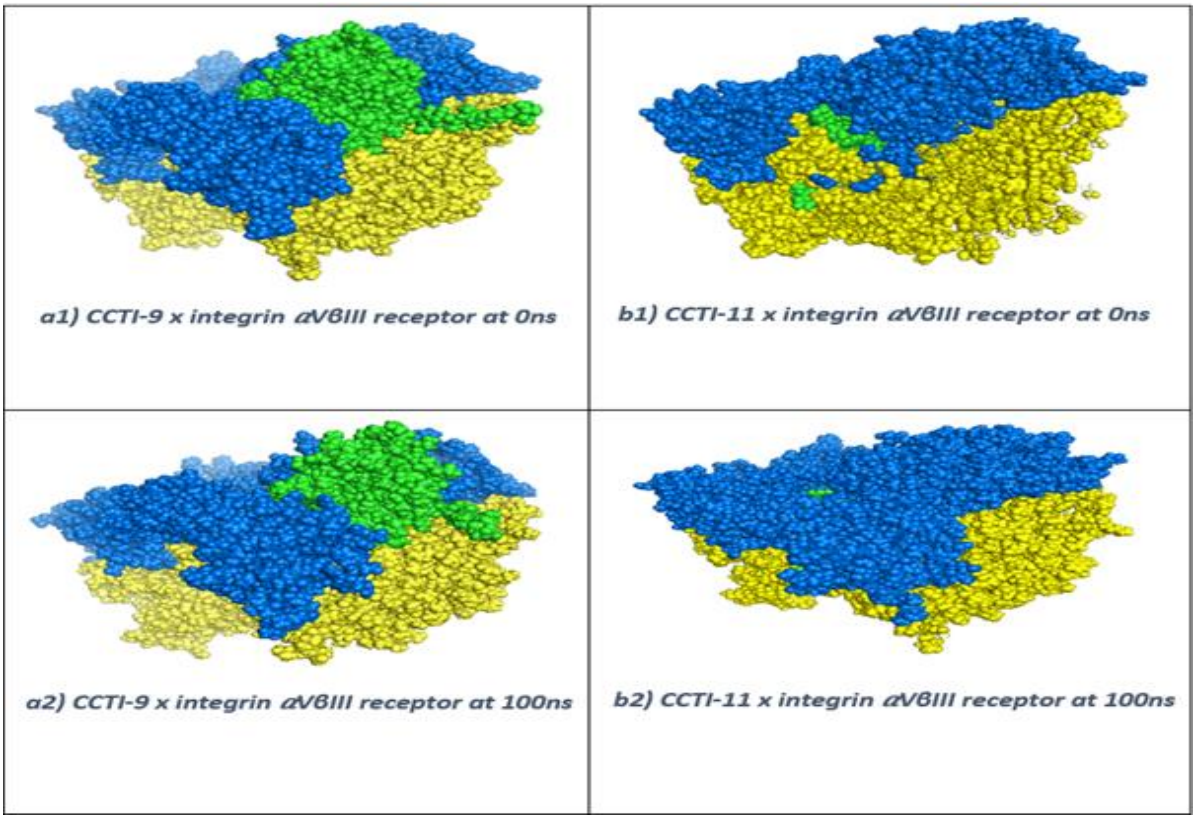

Figure 10: Superimposition of CcTI-9 x integrin αVβIII and CcTI-11 x integrin αVβIII before (a1 and b1) and after (a2 and b2) molecular simulations (blue and green representing chains of integrin while green indicate CcTIs ligands)

Xi'an Shiyou Daxue Xuebao (Ziran Kexue Ban)/
Journal of Xi'an Shiyou University, Natural Sciences Edition
ISSN: 1673-064X
E-Publication: Online Open Access
Vol: 67 Issue 12 | 2024
DOI: 10.5281/zenodo.14550712

The statistics from the simulation trajectory revealed the avg. rmsd values for unbounded CcTI-9 and CcTI-11 were 0.789nm and 0.359nm while integrin αVβIII receptor had rmsd of 0.441nm. The avg. rmsd values of the bounded CcTI-9 x integrin αVβIII and CcTI-11 x integrin αVβIII complexes were 0.833nm and 0.342nm (Fig. 11a1 and 11b1). Superimposition of rmsd spectra of native and docked CcTI-9, CcTI-11 and integrin receptor predicted CcTI-9 to have a greater variation, forming a relatively unstable composite with integrin. Interestingly, a lowered rmsd and slight deviation of CcTI-11 docked complex (Fig. 11b1) indicated stable and consistent complex with integrin.

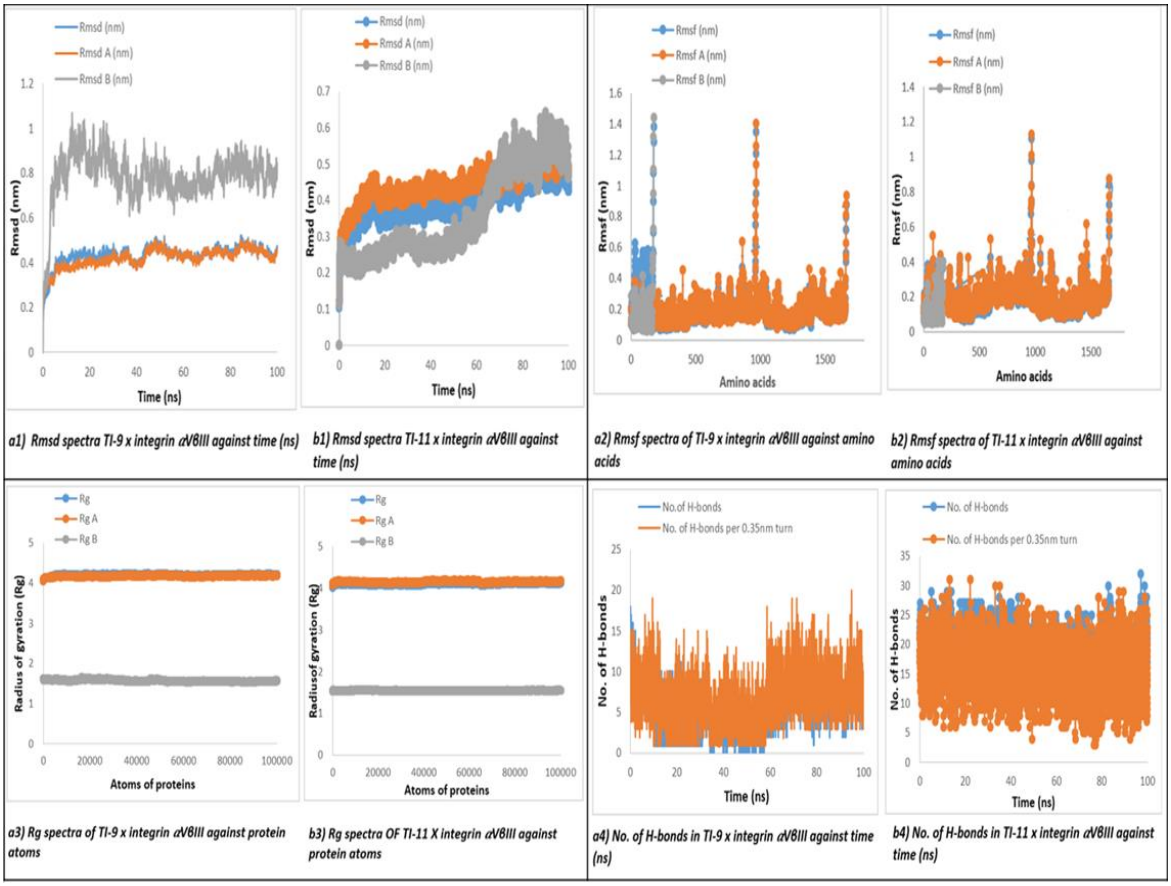

Figure 11: Superimposition of rmsd spectra of native CcTI -9, CcTI-11 and integrin αVβIII receptor with spectra of docked complexes (CcTI-9 x integrin αVβIII and CcTI-11 x integrin αVβIII) versus time (Fig. 9a1 and 9b1), Superimposition of rmsf spectra of native CcTI -9, CcTI-11 and integrin αVβIII receptor with spectra of docked complexes versus time (Fig. 9a2 and 9b2), Superimposition of spectra of average value of radius of gyration (Rg) native CcTI -9, CcTI-11 and integrin αVβIII receptor with spectra of docked complexes versus the atomic residues of proteins (Fig. 9a3 and 9b3), and superimposition of the spectra indicating average no. of hydrogen bonds of native CcTI -9, CcTI-11 and integrin αVβIII receptor with spectra of docked complexes versus time (Fig. 9a4 and 9b4)

Xi'an Shiyou Daxue Xuebao (Ziran Kexue Ban)/
Journal of Xi'an Shiyou University, Natural Sciences Edition
ISSN: 1673-064X
E-Publication: Online Open Access
Vol: 67 Issue 12 | 2024
DOI: 10.5281/zenodo.14550712

The fluctuations in binding residues of the ligand and receptor are analyzed to determine the variation in the protein's active site. The avg. rmsf values of unbounded CcTI-9, CcTI-11, and integrin αVβIII receptor were 0.177, 0.112, and 0.183.

However, the avg. rmsf values for CcTI-9 x integrin αVβIII and CcTI-11 x integrin αVβIII docked complexes were 0.186 and 0.126 (Fig. 11a2 and 11b2). A significant fluctuation at 150-170 amino acid residual positions at the C-terminal of CcTI-9 was observed as a distinct variable peak (Fig. 11a2), however, CcTI-11 had a continuous display with only a slight noticeable flexibility in the plot (Fig. 11b2).

To study the compactness and conformational stability of protein before and after docking, radius of gyration predicted no significant increase or decrease in CcTI-9 and CcTI-11 complexes with integrin (Fig. 11a3 and 11b3). The unbounded CcTI-9 had an avg. Rg value of 3.057nm is slightly higher than the 3.64 value of free CcTI-11. However, the docked complex of CcTI-9 showed an avg. Rg value of 4.2, whereas, the CcTI-11 docked complex had a gyration of 4.1.

A comparative continuous pattern was seen in Rg values with nearly 4.1nm, whereas, the unbounded CcTI-9 and CcTI-11 had quite a low Rg value of 1.8nm than the bound ones (Fig. 11a3 and 11b3). This stability in the docked CcTI-9 and CcTI-11 suggested accurate binding of ligands with integrin αVβIII receptor. The no. of hydrogen bonding was higher in CcTI-11 x integrin αVβIII (i.e. >30) compared to CcTI-9 x integrin αVβIII (<20). Thus, CcTI-11 was proposed to exhibit better inter and intra-molecular interactions.

The no. of hydrogen bonding was higher in CcTI-11 x integrin αVβIII in comparison to CcTI-9 x integrin αVβIII. The hydrogen bond interaction (Table 7) distances were monitored and plotted versus time (Fig. 11a4 and 11b4) (Gogoi *et al*., 2021). The numerical data of simulation parameters is given in the supporting information attached.

Table 11: Simulations data for rmsd, rmsf, Rg value, and no. of hydrogen bonds FOR CcTI-9, CcTI-9 x integrin αVβIII, CcTI-11, and CcTI-11 x integrin αVβIII

Simulations parameters	CcTI-9	CcTI-9 x integrin αVβIII	CcTI-11	CcTI-11 x integrin αVβIII
Rmsd (nm)	0.789nm	0.833nm	0.359nm	0.342nm
Rmsf (nm)	0.177nm	0.186nm	0.112nm	0.126nm
Radius of gyration (Rg)	3.057nm	4.2nm	3.64nm	4.1nm
Hydrogen bonds	>20	<20	~30	>30

Based on a series of insilico analysis homology modeling, protein-protein docking, PDBePISA evaluation, and stability graphics of molecular dynamic simulations, we propose CcTI-11 (accession no. >trIAOA151QRM2: MFTLFLLCALTSAIADAMVTDRDGDALRNGGTYHILPLFGVKDGGIELATTGNESCPLS VVQSPSGATFRGLPIRISSPYRVAYISEGLILSLAFASAPSCAPSPPKWTVVKGLPEGEA VKLPGYRSTVSGWFKIEKSSFEYLYKVVFCARGSDTCGDVGVSVDGGGVSRLVVTDD EGIFVEFMKGNSVDA) as a potential inhibitor of pro-cancerous integrin αVβIII receptor from a list of 12 different *Cajanus cajan* trypsin inhibitor proteins.

Xi'an Shiyou Daxue Xuebao (Ziran Kexue Ban)/
Journal of Xi'an Shiyou University, Natural Sciences Edition
ISSN: 1673-064X
E-Publication: Online Open Access
Vol: 67 Issue 12 | 2024
DOI: 10.5281/zenodo.14550712

As it is clearly known that the designing and development of novel therapeutic drugs is quite a lengthy, time-consuming, and expensive process, so, a combination of computational screening methodologies like structure prediction, protein-protein docking, simulation studies, and binding energy calculations are the earliest approaches to contribute in identifying potential drug candidates from compound libraries and databases (Ahmad *et al*., 2022). Such insilico predictions needs validation and support by invitro experiments of molecular cloning and biological assays confirming the therapeutic role of proteins as proposed by bioinformatics tools.

4. CONCLUSION AND FUTURE PROSPECT

Therapeutics and drug designing are practical fields with a constant hunt for new drug alternatives is highly supportive of carrying out the initial insilico investigative trials on the structural and biological properties of different biomolecules. The same approach was applied to 12 *Cajanus cajan* trypsin inhibitors (CcTIs).

The current bioinformatics knowledge of the molecular and cellular roles of trypsin inhibitors with different cell surface receptors gives researchers the drive to explore the potential interactions between inhibitors and adhesion molecules.

Overexpression of certain cell surface receptors under carcinogenesis hints towards their involvement as precancerous entities. From our study, we can conclude that trypsin inhibitors from *C. cajan* are promising anti-cancer drug targets against a variety of cancer cells bearing tumor prognostic receptors like integrin.

The molecular signaling pathway of trypsin inhibitors with integrin receptor gives insights that the inhibitor drug mimics the same behavior intracellular as depicted computationally. Thus, insilico analysis carried out on plant proteins, such as trypsin inhibitors leads to the early prediction of their in vitro protein function.

The full potential of any biological molecule cannot be determined purely on insilico basis, the computational findings need to be validated by invitro studies. This relative importance and balance of insilico and in vitro results is crucial to clinically address the biological nature of any newly identified plant-derived therapeutic agent. Thus, the role of structural biology always facilitates the investigations of functional biology of different biological macromolecules like proteins.

Acknowledgement

Higher Education Commission (HEC), Islamabad, Pakistan.

University of the Punjab.

Centre for Applied Molecular Biology (CAMB), University of the Punjab, Lahore.

Dr. Muhammad Bilal (Centre for Applied Molecular Biology, University of the Punjab, Lahore) and Mian Muhammad Mubashir (Punjab University College of Information Technology, University of the Punjab, Lahore).

ISSN: 1673-064X
E-Publication: Online Open Access
Vol: 67 Issue 12 | 2024
DOI: 10.5281/zenodo.14550712

Funding: This research did not receive any specific grant from funding agencies in the public, commercial, or not-for-profit sectors.

'Declaration of interest: 'None'

References

1) Clara, J.A., Monge, C., Yang, Y., & Takebe, N., 2020. Targeting signalling pathways and the immune microenvironment of cancer stem cells—A clinical update. Nat. Rev. Clin. Oncol. 17, 204-232.

2) Cheng, S.S., Jun Yang, G.J., Wang, W., Leung, C.H., & Ma, D.K., 2020. The design and development of covalent protein-protein interaction inhibitors for cancer treatment. J. Hematol. Oncol. 13, 1-14.

3) Abu-Darwish, MS., & Efferth, T., 2018. Medicinal plants from near east for cancer therapy. Front. Pharmacol. 9, 302475.

4) Soreide, K., Janssen, E.A., Korner, H., Baak, J.P., 2006. Trypsin in colorectal cancer: molecular biological mechanisms of proliferation, invasion, and metastasis. J. Pathol. 209, 147-56.

5) Rasouli, H., Parvaneh, S., Mahnam, A., Rastegari-Pouyani, M., Hoeinkhani, Z., Mansouri, K., 2017. Anti-angiogenic potential of trypsin inhibitor purified from Cucumis melo seeds: Homology modeling and molecular docking perspective. Int. J. Biol. Macromol. 96, 118-128.

6) De Paula, C.A., Coulson-Thomas, V.J., Ferreira, J.G., Maza, P.K., Suzuki, E., Nakahata, A.M., Nader, H.B., Sampaio, M.U., Olivia, M.L., 2012. Enterolobium contortisiliquum trypsin inhibitor (EcTI), a plant proteinase inhibitor, decreases in vitro cell adhesion and invasion by inhibition of Src protein-focal adhesion kinase (FAK) signaling pathways. J. Biol. Chem. 287, 170-182.

7) Rastija, V., Vrandecic, K., Cosic, J., Majic, I., Saric, G.K., Agic, D., Karnas, M., Loncaric, M., Molnar, M., 2021. Biological activities related to plant protection and environmental effects of coumarin derivatives: QSAR and molecular docking studies. Int. J. Mol. Sci. 14, 7283.

8) Castrosanto, M.A., Clemente, A.J., Whitefield, A.E., Alviar, K.B., 2023. In silico analysis of the predicted protein-protein interaction of syntaxin-18, a putative receptor of Peregrinus maidis Ashmead (Hemiptera: Delphacidae) with Maize mosaic virus glycoprotein. J. Biomol. Struct. Dyn. 41, 3956-3963.

9) Kumara, M., Kumarb, V., Kansalc, R., Srivastavad, P.S., Koundalc, K.R., 2016. Isolation and characterization of a novel gene encoding Kunitz-type protease inhibitor from Pigeon pea (Cajanus cajan L.). Eco. Env. & Cons. 22, 329-337.

10) Shamsi, T.N., Parveen, R., Afreen, S., Azam, M., Sen, P., Sharma, Y., Haque, Q.M., Fatma, T., Manzoor, N., Fatima, S., 2018. Trypsin Inhibitors from *Cajanus cajan* and *Phaseolus limensis* Possess Antioxidant, Anti-Inflammatory, and Antibacterial Activity. J. Diet. Suppl. 15, 939-950.

11) Shamsi, T.N., Parveen, R., Ahamad, S., Fatima, S., 2017. Structural and biophysical characterization of Cajanus cajan protease inhibitor. J. Nat. Sci. Biol. Med. 8, 186.

12) Yousafi, Q., Kanwal, S., Rashid, H., Khan, M.S., Saleen, S., Aslam, M., 2019. In silico structural and functional characterization and phylogenetic study of alkaline phosphatase in bacterium, Rhizobium leguminosarum (Frank 1879). Comp. Bio. Chem. 83, 107142.

13) Mahmoud, A., Kotb, E., Alqosaibi, A.I., Al-Karmalawy, A.A., Al-Dhuayan, I.S., Alabkari, H., 2021. In vitro and in silico characterization of alkaline serine protease from Bacillus subtilis D9 recovered from Saudi Arabia. Heliyon. 7.

ISSN: 1673-064X
E-Publication: Online Open Access
Vol: 67 Issue 12 | 2024
DOI: 10.5281/zenodo.14550712

14) Afolabi, R., Chinedu, S., Ajamma, Y., Adam, Y., Koenig, R., Adebiyi, E., 2022. Computational identification of *Plasmodium falciparum* RNA pseudouridylate synthase as a viable drug target, its physicochemical properties, 3D structure prediction and prediction of potential inhibitors. Infect. Genet. Evol. 97, 105194.

15) Hossain, M.M., 2012. Fish antifreeze proteins: Computational analysis and physicochemical characterization. Int. Curr. Pharm. J. 1, 18-26.

16) Shey, R. A., Ghogomu, S. M., Nebangwa, D. N., Shintouo, C. M., Yaah, N. E., Yengo, B. N., . . . Mbachick, T. T. 2022. Rational design of a novel multi-epitope peptide-based vaccine against Onchocerca volvulus using transmembrane proteins. *Frontiers in Tropical Diseases*. **3**:1046522.

17) Zahid, E., and Sarwar, M. F. 2023. Multiple structural and functional annotations based in-silico characterization of Q9BRX8 protein. *Karbala International Journal of Modern Science*. **9**:18.

18) Madanagopal, P., Ramprabhu, N., Jagadeesan, R., 2022. In silico prediction and structure-based multitargeted molecular docking analysis of selected bioactive compounds against mucormycosis. 46, 24.

19) Xu, J., 2019. Distance-based protein folding powered by deep learning. PNAS. 116, 16856-16865.

20) Anishchenko, Beak, M., Park, H., Hiranuma, N., Kim, D.E., Dauparas, J., Mansoor, S., Humphreys, I.R., Baker, D., 2021. Protein tertiary structure prediction and refinement using deep learning and Rosetta in CASP14. Proteins:Struct. Funct. Genet. 89, 1722-1733.

21) Hasan, R., Rony, M.N.H., Ahmed, R., 2021. In silico characterization and structural modeling of bacterial metalloprotease of family M4. J. Genet. Eng. Biotechnol. 19, 25.

22) Saleem, S., Khan, A., Ali, S.S., Sayaf, A.M., Khan, M., Molecular modeling of the multiple-drug resistant protein (MRP7) and pharmacophore modelling based virtual screening to identify novel drugs against cancer. J. Comput. Chem. 230027.

23) Singh, N., Dalal, V., Kumar, V., Sharma, M., Kumar, P., 2019. Characterization of phthalate reductase from Ralstonia eutropha CH34 and in silico study of phthalate dioxygenase and phthalate reductase interaction. J. Mol. Graphics Modell. 90, 161-170.

24) Dong, S., Lau, V., Song, R., lerullo, M., Esteban, E., Wu, Y., Sivieng, T., Nahal, H., Gaudinier, A., Pasha, A., 2019. Proteome-wide, structure-based prediction of protein-protein interactions/new molecular interactions viewer, J. Plant Physiol. 179, 1893-1907.

25) Aguiar, J. R. d. S. B, 2021. Doctoral dissertation. Univ. Sao Paulo. 13122021-161816.

26) Gaur, M., Tiwari, A., Chauhan, R.P., Pandey, D., Kumar, A., 2018. Molecular modeling, docking and protein-protein interaction analysis of MAPK signalling cascade involved in Camalexin biosynthesis in Brassica rapa. Bioinformation. 14, 145.

27) Iqbal, A., Latif, A., Galbraith, D.W., Jabbar, B., Ali, M.A., Ahmed, M., Gul, A., Rao, A.Q., Shahid, A.A., Husnain, T., 2021. Structure-based prediction of protein–protein interactions between GhWlim5 Domain1 and GhACTIN-1 proteins: a practical evidence with improved fibre strength. J. Plant Biochem. Biotechnol. 30, 373-386.

28) Uciechowska-Kaczmaryck, U., de Beauchene, I.C., Samsonov, S.A., 2019. Docking software performance in protein-glycosaminoglycan systems. J. Mol. Graphics Modell. 90, 42-50.

29) Roy, A., Menon, T., 2022. Evaluation of bioactive compounds from *Boswellia serrata* against SARS-CoV-2. Vegetos. 35, 404-414.

30) Yan, Y., Tao, H., He, J., Huang, S.Y., 2020. The HDOCK server for integrated protein–protein docking. Nat. Protoc. 1, 1829-1852.

ISSN: 1673-064X
E-Publication: Online Open Access
Vol: 67 Issue 12 | 2024
DOI: 10.5281/zenodo.14550712

31) Scafuri, N., Soler, M.A., Spitaleri, A., Rocchia, W., 2021. Enhanced molecular dynamics method to efficiently increase the discrimination capability of computational protein–protein docking. J. Chem. Theory Comput. 7, 7271-7280.

32) Rosell, M., Fernandez-Recio, J., 2020. Docking approaches for modeling multi-molecular assemblies. Curr. Opin. Struct. Biol. 64, 59-65.

33) Arya, H., 2021. In silico validation through protein-protein docking. Elsevier. 121-132.

34) Krissinel, E., Henrick, K., 2007. Inference of macromolecular assemblies from crystalline state. J. Mol. Biol. 372, 774-797.

35) Suganthi, M., Sowmya, H., Manjunathan, J., Ramasamy, P., Thiruvengadam, M., Varadharajan, V., Venkidasamy, B., Senthilkumar, P., 2024. Homology modeling and protein-protein interaction studies of GAPDH from Helopeltis theivora and chitinase from Pseudomonas fluorescens to control infection in tea [Camellia sinensis (L.) O. Kuntze] plants. Plant Stress. 11, 100377.

36) Das, P., Majumder, R., Mandal, M., Basak, P., 2021. In-Silico approach for identification of effective and stable inhibitors for COVID-19 main protease (Mpro) from flavonoid based phytochemical constituents of Calendula officinalis. J. Biomol. Struct. Dyn. 39, 6265-6280.

37) Majumder, R., Mandal, M., 2022. Screening of plant-based natural compounds as a potential COVID-19 main protease inhibitor: an in silico docking and molecular dynamics simulation approach. J. Biomol. Struct. Dyn. 40, 696-711.

38) Eleftheriou, P., Amanatidou, D., Petrou, A., Geronikaki, A., 2020. In silico evaluation of the effectivity of approved protease inhibitors against the main protease of the novel SARS-CoV-2 virus. Molecules. 25, 2529.

39) Haq, S.K., Khan, R.H., 2003. Characterization of a proteinase inhibitor from Cajanus cajan (L.). J. Protein. Chem. 22, 543-554.

40) Swathi, M., Lokya, V., Swaroop, V., Mallikarjuna, N., Kannan, M., Dutta-Gupta, A., Padmasree, K., 2014. Structural and functional characterization of proteinase inhibitors from seeds of Cajanus cajan (cv. ICP 7118). Plant Physiol. Biochem. 83, 77-87.

41) Cid-Gallegos, M.S., Corzo-Rios, L.J., Jimenez-Martinez, C., Sanchez-Chino, X.M., 2022. Protease inhibitors from plants as therapeutic agents-a review. Plant Foods Hum. Nut. 77, 20-29.

42) Leppkes, J., 2022. Doc. Diss.

43) Jumper, J., Evans, R., Pritzel, A., Green, T., Figurnov, M., Ronneberger, O., Tunyasuvunakool, K., Bates, R., Zadek, A., Potapenko, A., Bridgland, A., 2021. Highly accurate protein structure prediction with AlphaFold. Nature. 596, 583-589.

44) de Medeiros, A.F., de Souza, B.B., Coutinho, L.P., Murad, A.M., Dos Santos, I.P., Monteiro, N.D., Santos, E.A., Maciel, B.L., Araujo Morais, A.H., 2021. Structural insights and molecular dynamics into the inhibitory mechanism of a Kunitz-type trypsin inhibitor from Tamarindus indica L. J. Enzyme Inhib. Med. Chem. 36, 480-490.

45) Weis, S.M., Cheresh, D.A., 2011. αV integrins in angiogenesis and cancer. Cold Spring Harb. Perspect. med. 1, a006478.

46) Ludwig, B.S., Kessler, H., Kossatz, S., Reuning, U., 2021. RGD-binding integrins revisited: how recently discovered functions and novel synthetic ligands (re-) shape an ever-evolving field. Cancers. 13, 1711.

47) Mahnam, H.R.S.P.A., 2016. Anti-angiogenic potential of trypsin inhibitor purified. angiogenesis. 1, 11-12.

ISSN: 1673-064X
E-Publication: Online Open Access
Vol: 67 Issue 12 | 2024
DOI: 10.5281/zenodo.14550712

48) Nielsen, N.S., Zarantonello, A., Harwood, S.L., Jensen, K.T., Kjoge, K., Thogersen, I.B., Schauser, L., Karlsen, J.L., Andersen, G.R., Enghild, J.J., 2022. Cryo-EM structures of human A2ML1 elucidate the protease-inhibitory mechanism of the A2M family. Nat Commun. 13, 3033.

49) Gartia, J., Barnwal, R.P., Chary, K.V., 2020. Statistical analysis of intermolecular interactions in trypsin-inhibitor complexes. J. Biomol. Struct. Dyn. 38, 5287-5292.

50) Gogoi, B., Chowdhury, P., Goswami, N., Gogoi, N., Naiya, T., Chetia, P., Mahanta, S., Chetia, D., Tanti, B., Borah, P., Handique, P.J., 2021. Identification of potential plant-based inhibitor against viral proteases of SARS-CoV-2 through molecular docking, MM-PBSA binding energy calculations and molecular dynamics simulation. Molecular diversity. 25, 1963-1977.

51) Ahmad, S., Bhanu, P., Kumar, J., Pathak, R. K., Mallick, D., Uttarkar, A., ... & Mishra, V. 2022. Molecular dynamics simulation and docking analysis of NF-κB protein binding with sulindac acid. Bioinformation, 3, 170.